MHD 1996
Yokohama

DEVELOPMENT OF A MHD CODE USING CIP METHOD AND ITS APPLICATION TO ICF ROCKET

Yoshihiko Nagamine, Tomokazu Fusuki, Yuji Nakama, Takao Mayumi,
and Hideki Nakashima
Department of Energy Conversion Engineering, Kyushu University
Kasuga, Fukuoka 816, Japan

Abstract

A magnetohydrodynamics (MHD) code is developed. CIP (cubic interpolated pseudo particle) method is used to solve hydrodynamics, density function method is adopted to trace the plasma surface as a free boundary, and SSI (symmetrical semi-implicit) method is used to calculate the diffusion term. The code is checked against the following problems: (i) cylindrical shock tube, (ii) converging cylindrical shock, and (iii) unsteady flow into a vacuum. Furthermore, the code is checked against the heat wave propagation for non-linear heat conduction and MHD shock. We found good agreement between the self-similar solutions and the numerical results. The analysis of the plasma behavior in the magnetic nozzle is performed for a fusion rocket. The results of the code show a plasma behavior consistent with the magnetic nozzle concept. However the conservation of plasma mass is not good, so that the estimation of the thrust conversion efficiency is subject to ambiguity that must be removed by further investigation.

1. Introduction

Fusion reaction can release a large amount of energy. To give rise to the fusion reaction, two schemes are proposed. One is magnetic confinement fusion (MCF) and the other is inertial confinement fusion (ICF). Use of energy released by fusion could realize a propulsion system that might be more attractive compared with existing systems. A propulsion system driven by a laser-induced fusion, so called ICF rocket, is an attractive candidate. It could provide both large specific impulse and power. Design studies of spacecraft based on ICF have been made for several years by some researchers. [1, 2]

The basic concept of ICF rocket is as follows: ICF rocket has a magnetic nozzle composed of a solenoidal superconducting magnet. When the fusion reaction occurs by laser irradiation of pellet, the resulting plasma as fusion products begins to expand into the external magnetic field. The plasma compresses the magnetic field and deposits its energy to the magnetic field. As the plasma reaches the maximum expansion radius, the compressed magnetic field starts to push back the plasma and redirect it, thus producing thrust.

In order to indicate the validity of the above concept, analysis of the plasma behavior in the magnetic nozzle and the estimation of the thrust conversion efficiency have been performed. For example, Hyde [1] has proposed a conceptual design of ICF rocket and has calculated the thrust conversion efficiency by using magnetohydrodynamics (MHD) code. The efficiency was reported to be 60 % there. However the efficiency depends on the configuration of the magnetic nozzle, i.e., the intensity or shape of magnetic field, fusion reaction point, etc. Thus parametric research is needed to find the optimum configuration of the nozzle and to obtain the thrust conversion efficiency.

A new MHD code is being developed by the present authors. The code uses CIP (Cubic Interpolated Pseudo Particle) method [3] to analyze the plasma behavior in the magnetic nozzle. The CIP method is a universal solver for hyperbolic equation and its characteristics is numerically stable and less diffusive.

When calculating the plasma expansion into a magnetic field in the magnetic nozzle, the plasma cloud initially occupies a small region of the whole

calculational domain and then it expands rapidly outward. This requires a robust and stable computation method. This is the reason why the CIP method is adopted here for the analysis of plasma behavior in the magnetic nozzle.

The plan of the present paper is as follows: In the next section the basic equation of the plasma motion and description of the computational model are presented. In section 3, the code is checked against the well known problems of fluid dynamics: (i) shock tube [3], (ii) cylindrical converging shock [4], and (iii) unsteady flow into a vacuum [5]. The analysis of plasma behavior in the magnetic nozzle is presented in section 4 along with discussions. The model adopted here is based on a configuration proposed by Hyde. [1] The conclusion is given in section 5.

2. Computational Model

2.1 Basic Equation

Basic equations solved in the present simulation code are the following one-fluid MHD equations and Maxwell equations in MKS units.

$$\frac{\partial \rho}{\partial t} + u \cdot \nabla \rho + \rho \nabla \cdot u = 0, \tag{1}$$

$$\frac{\partial u}{\partial t} + u \cdot \nabla u + \frac{1}{\rho}(\nabla p - J \times B) = 0, \tag{2}$$

$$\frac{\partial T}{\partial t} + u \cdot \nabla T + \frac{1}{\rho C_v}(p(\nabla \cdot u) - E \cdot J) = \frac{1}{\rho C_v}((\nabla \cdot (\kappa \nabla T)), \tag{3}$$

$$J = \frac{1}{\mu_0} \nabla \times B, \tag{4}$$

$$\nabla \times E = -\frac{\partial B}{\partial t}. \tag{5}$$

Here, ρ is the density of plasma, u the velocity, p the pressure, J the current density, B the magnetic field intensity, T the temperature, C_v the specific heat, E the electric field intensity, κ the heat conductivity, and μ_0 the permeability of free space. The plasma density n and the pressure p represent $(n_i + n_e)$ and $(p_i + p_e)$, respectively. Furthermore the generalized ohm's law is used:

$$E = -u \times B + \eta \cdot J - \frac{\nabla p_e}{n_e}, \tag{6}$$

where η is the electric conductivity. The subscript i and e attached to p and n denote the components of the ion and electron, respectively.

2.2 Description of Model and Method

The code treats the compressible flow as given in equation (1). Cylindrical symmetry is assumed: $2\frac{1}{2}$-dimensional $(r, z, v_r, v_\theta, v_z; \frac{\partial}{\partial \theta} = 0)$ model is adopted here.

Introducing the magnetic vector potential ($\nabla \times A = B$) in the Coulomb gauge, and utilizing the equation (6), we obtain the equation

$$\frac{\partial A}{\partial t} = u \times (\nabla \times A) - \frac{\eta}{\mu_0} \nabla \times (\nabla \times A) + \frac{\nabla p_e}{n_e}, \tag{7}$$

where the relation $E = -\frac{\partial A_\theta}{\partial t}$ has been used. Taking the rotation of the equation (6) and substituting the resulting equation into the equation (5), we obtain the following equation,

$$\frac{\partial B}{\partial t} = \nabla \times (u \times B) + \nabla \times (\frac{\eta}{\mu_0} \nabla \times B) - \nabla \times (\frac{\nabla p_e}{n_e}). \tag{8}$$

Thus B_r and B_z can be obtained from the θ component of equation (7) and B_θ is given by the θ component of the equation (8).

As mentioned previously, the CIP [3] method is adopted here. The CIP method is proposed to solve the fluid equation which has the form,

$$\frac{\partial f}{\partial t} + (u \cdot \nabla) f + G = H, \tag{9}$$

where

$$f = (\rho, u, T), \tag{10}$$

$$G = (\rho \nabla \cdot u, \frac{1}{\rho}(\nabla p - J \times B), \frac{1}{\rho C_v}(p(\nabla \cdot u) - E \cdot J)), \tag{11}$$

$$H = (0, 0, \frac{1}{\rho C_v}(\nabla \cdot (\kappa \nabla T))). \tag{12}$$

In this method, equation (9) is sequentially solved in time,

$$\frac{\partial f}{\partial t} = H, (\text{diffusion phase}), \tag{13}$$

$$\frac{\partial f}{\partial t} = -G, (\text{non-advection phase}), \tag{14}$$

and

$$\frac{\partial f}{\partial t} + (u \cdot \nabla) f = 0, (\text{advection phase}). \tag{15}$$

The CIP method is applied to the equations(15): this equation is solved by shifting a cubic-interpolated profile with a local velocity u. On the other hand, the equations(14) can be solved using the finite difference method. For the equations(13), SSI (Symmetrical Semi-Implicit scheme) method [6] is applied. Furthermore, the

same procedure is adopted in solving the equations (7) and (8).

When the plasma expands into the magnetic field in the magnetic nozzle, the surface of the plasma faces a vacuum. In the present situation, the discontinuity of the density would appear between the plasma and vacuum. Thus, to treat the plasma surface as a free boundary, we adopt the density function method [7]. The definition of the density function ϕ is as follows:

$$\phi = \begin{cases} 0, & \text{for the vacuum} \\ 1. & \text{for the plasma} \end{cases}$$

The plasma surface locates in the region $0 < \phi < 1$. This density function evolves according to the equation,

$$\frac{\partial \phi}{\partial t} + u \cdot \nabla \phi = 0. \qquad (16)$$

However, as proposed in the reference [7], in order to avoid diffusion and oscillation in the CIP method, we introduce a new function F_ϕ,

$$F_\phi = \tan[0.99\pi(\phi - 0.5)], \qquad (17)$$

which is a function of ϕ only. Hence, we solve the equation,

$$\frac{\partial F_\phi}{\partial t} + u \cdot \nabla F_\phi = 0, \qquad (18)$$

instead of the equation(16) to trace the plasma surface effectively.

3. Application to Problems

We checked the code against the well-known problems of the fluid dynamics: (i) cylindrical shock tube [3], (ii) converging cylindrical shock [4], and (iii) unsteady flow into a vacuum [5]. In addition to the above problems, we also checked the heat wave propagation for non-linear heat conduction [8] and MHD shock problem [9].

3.1 Cylindrical Shock Tube

The cylindrical shock tube problems in both low Mach number and high Mach number regimes are checked. The initial condition in the low Mach number regime is $\rho = 1$ and $p = 1$ for the left most 200 zones and $\rho = 0.125$ and $p = 0.1$ for the other zones; $u = 0$ and $\gamma = 1.4$ in all zones with the grid size $\Delta x = 0.005$ and time interval $\Delta t = 0.005$. In the high Mach number regime, the initial condition is $\rho = 1.0$ and $p = \frac{2}{3}$ for the left most 200 zones and $\rho = 0.5$ and $p = 0.5 \times 10^{-4}$ for the other zones; $u = 0$ and $\gamma = \frac{5}{3}$ in all zones with $\Delta x = 1.0$ and $\Delta t = 0.1$. The numerical results both in the low and high Mach number regimes showed good agreement with the analytical results [3].

3.2 Converging Cylindrical Shock

As shown in Fig.1, the initial conditions are set as follows [4]: ρ and p in the inner region ($0 < r < 1$) are set equal to 1.0 and the corresponding quantities in the outer region ($1 < r < 2$) are set equal to 4.0, and $u = 0$ in the both regions with $\Delta r = 0.02$ and $\Delta t = 0.5 \times 10^{-3}$.

In Fig.1, the pressure distributions are displayed at a time interval of 0.2. It is found that the shock propagates towards the axis with increasing time, then the shock reaches the axis, and it is reflected outward.

We found good agreement between the results of the present code and other numerical calculations [4].

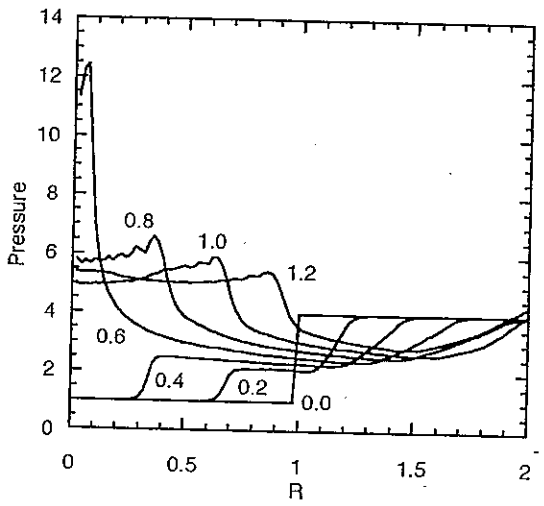

Fig.1 Pressure distribution at a time interval of 0.2

3.3 Unsteady Flow into A Vacuum

Introducing the density function method in the section 2, we checked the method against the unsteady flow into a vacuum [5].

We gave the density and pressure profiles as the initial conditions; $\rho = 1$ and $p = 0$ for the right most 200 zones and $\rho = 0$ and $p = 0$ for the other zones; $u = 0$ in all zones. The other parameters are $\gamma = 1.4$, $\Delta x = 0.2$ and $\Delta t = 0.5 \times 10^{-6}$.

Then the results of the code are compared with the analytical solutions [5],

$$\rho = \rho_0[1 - \frac{\gamma - 1}{2}\frac{|u|}{C_0}]^{2/(\gamma-1)},$$

$$p = p_0[1 - \frac{\gamma - 1}{2}\frac{|u|}{C_0}]^{2\gamma/(\gamma-1)},$$

$$|u| = \frac{2}{\gamma+1}(C_0 - \frac{x}{t}),$$

where C is the sound speed and the subscription 0 denotes the initial value.

Figure 2 gives the results of the code. The results showed good agreement with the analytical solutions, except in low density region. The code neglects the low density region to avoid the divergence during the calculation.

Thus, it is found that the material surface is successfully traced by using the density function.

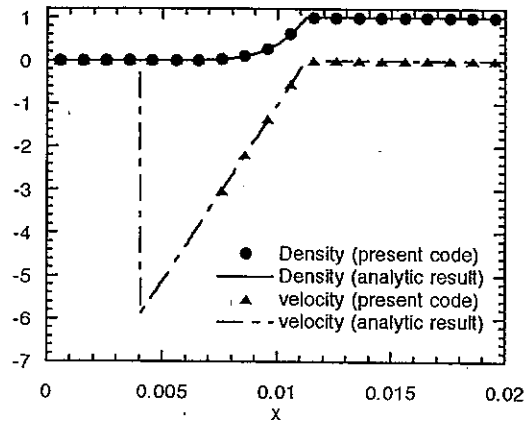

Fig.2 Density and velocity distributions

3.4 Non-linear Heat Conduction

In order to check the treatment at the diffusion phase of equation(13), we calculate a non-linear heat conduction through the medium which is called a Marshak Wave. The self similar solution for the plane medium with its fixed boundary temperature is as follows [8];

$$\chi_f = \sqrt{aT_0^3 l_R \cdot ct/2.28\rho C_v}, \qquad (19)$$

where χ_f is the position of the wave front, T_0 the initial boundary temperature, l_R the Rosseland mean free path, c the speed of light, t the time and ρ the density of medium. The equation(19) can be written [8],

$$\chi_f \propto \sqrt{t}, \qquad (20)$$

for a given density and temperature.

The initial conditions adopted here are $T_0 = 5.0 \times 10^6$ K and $\rho = 1.13 \times 10^4$.

The results of the code are shown in Fig.3 and Fig.4. Figure 3 gives a propagation of the Marshak Wave as a function of time. It is seen that

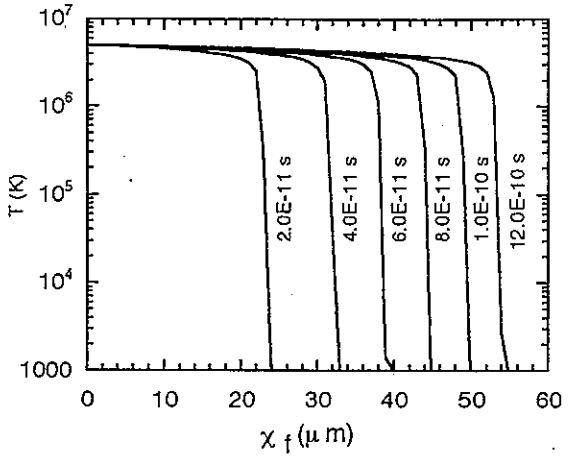

Fig.3 Propagation of a Marshak Wave for a boundary temperature of $5 \times 10^6 K$

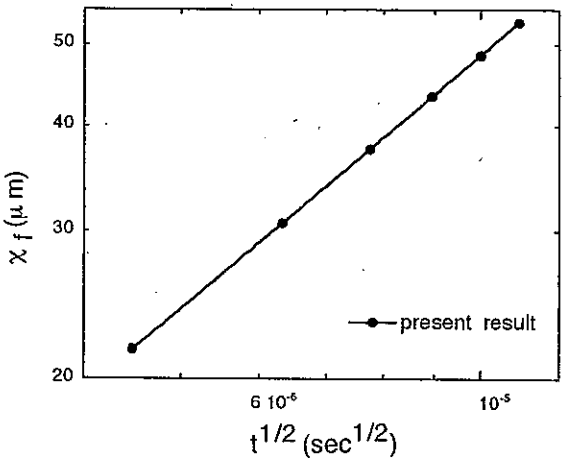

Fig.4 Plot of χ_f against $\sqrt{t}$

the wave slows down with time as predicted by the equation(19). The χ_f against $\sqrt{t}$ is plotted in Fig.4. The solid line represents the code results and it is consistent with the equation(20).

3.5 MHD Shock Problem

The MHD shock tube problem [9] is taken up to check the code against the magnetohydrodynamics problems. Here the frame of the code is changed from cylindrical coordinate to Cartesian one. We consider one-dimensional MHD equations for the code: All variables depend on x and t only.

The initial data consist of two constant states [9]: For the initial left regions, $\rho = 1$, $p = 1$, and $B_y = 1$. For the initial right regions, $\rho = 0.125$, $p = 0.1$, and $B_y = -1$. $u = 0$, $v = 0$ and $B_x = 0.75$ for all regions. The rest of parameters are $\gamma = 2$, $\Delta x = 1$ and $\Delta t = 0.2$. The initial hydrodynamical data used here are similar to those of the shock tube problems given in section 3.1.

The results of preliminary calculation showed qualitative agreements with those reported in reference [9].

4. Analysis of The Plasma Behavior in The Magnetic Nozzle

The calculational model for the magnetic nozzle adopted here is based on the design of ICF rocket proposed by Hyde [1].

A schematic layout of the magnetic nozzle is shown in Fig.5. The magnetic field in the nozzle is generated by a solenoidal SCM (superconducting magnet) coil which has a radius of 6.5 m , carries a current of 22 MA and stores 7978 MJ. An angle θ (cone angle) subtended from the Z axis to the solenoidal coil is taken to be 55°. The dimensions (R × Z) of the calculational region are 10m×20m. $\Delta t = 1.0\times10^{-11}$ sec and $\Delta x = 0.1$ m are adopted.

The plasma has a radius of 1 m and a mass of 8.3 g mainly contributed by hydrogen propellant. Its density distribution is uniform. The internal energy derived from fusion reaction is 1300 MJ.

The preliminary results by the code are shown in Fig.6 and Fig.7. Figure 6 gives a temporal change of magnetic field distribution. The external magnetic field is compressed by the expanding plasma, and then redirect it. On the other hand it can be seen from Fig.7 of density distribution that the plasma expands isotropicaly in the early stage while compressing the external magnetic field. Then, it is reflected by the external magnetic field shown in Fig.6.

The results of the code show a behavior of the plasma which is consistent with the magnetic nozzle concept mentioned in section 1. However, the estimation of the thrust efficiency is subject to ambiguity, because the conservation of the plasma mass is not good. This may be caused by inappropriate selection of Δt and Δx related to Courant-Friedrich-Lewy condition. Thus, further study is needed to obtain a final results of the thrust efficiency.

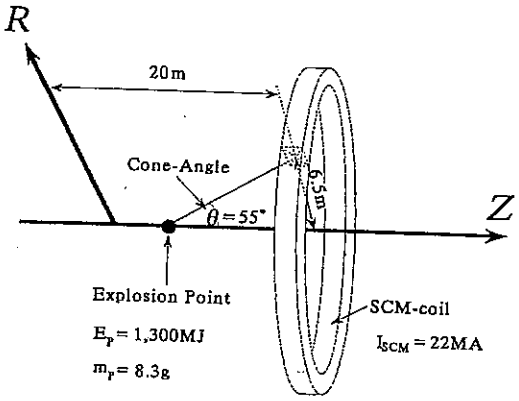

Fig.5 Schematic layout of the magnetic nozzle

5. Conclusions

We have develop a MHD code using a CIP method. In order to trace the plasma surface effectively, the density function method is adopted. The SSI method is used to solve a diffusion equation.

The code is checked against the problems of fluid dynamics: (i) cylindrical shock tube, (ii) converging cylindrical shock, and (iii) unsteady flow into a vacuum. We found good agreements between the results of the calculation by the present CIP code and the analytical or self-similar solutions. Furthermore, the code is checked against the heat wave propagation for non-linear heat conduction and MHD shock.

Analysis of plasma behavior in the magnetic nozzle is performed. The results of the code show a plasma behavior consistent with the magnetic nozzle concept. However, the conservation of the plasma mass is not good, so that the estimation of the thrust conversion efficiency is subject to ambiguity that must be removed by further investigation.

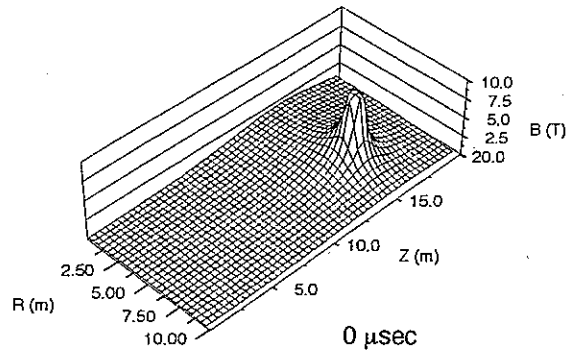

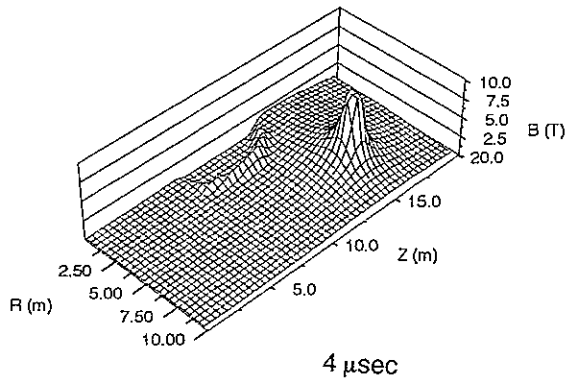

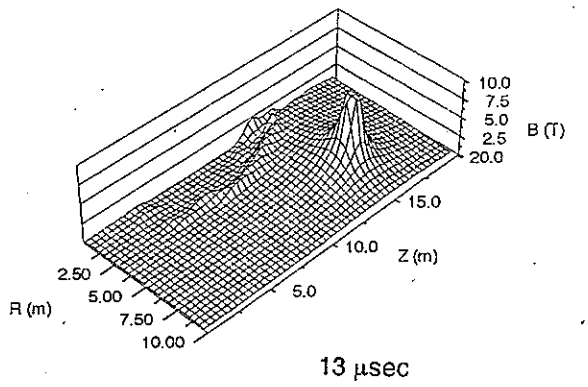

Fig.6 Temporal change of magnetic field. The time evolves from top to bottom.

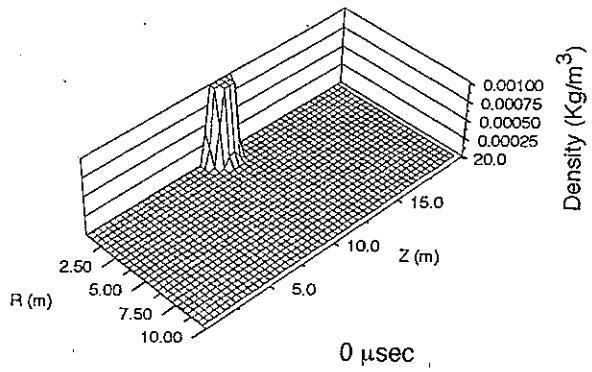

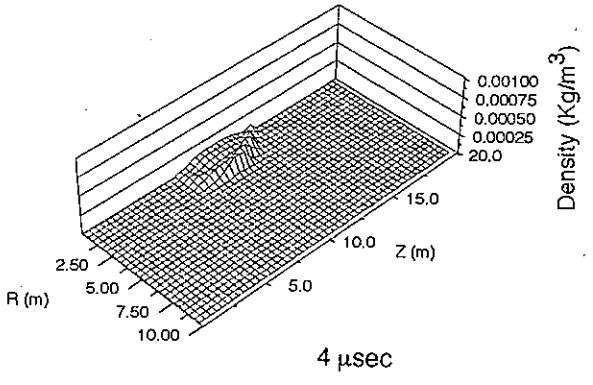

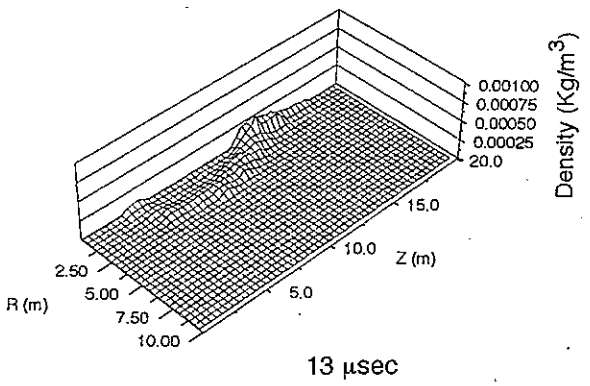

Fig.7 Temporal behavior of plasma in the magnetic field. The time evolves from top to bottom.

References

[1] Hyde, R. A., *UCRL-99957* (1983)

[2] Orth, C. D., *et al.*, *UCRL-96676 and UCRL-96832* (1987)

[3] Takewaki, H. and Yabe, T. *J. Comput Phys.*, **70**, pp.355-372 (1987)

[4] Sod, G. A., *J. Fluid Mech.*, **83** part 4, pp.785-794 (1977)

[5] Zel'dovich, Ya. B., *et al.*, *"Physics of Shock Waves and High Temperature Hydrodynamics Phenomena"*, Vol. I, Academic Press, New York (1966)

[6] Yabe, T. and Ishikawa, T., *NIFS-119* (1991)

[7] Yabe, T., and Xiao, F., *J. Phys. Soc. Jpn*, **62**, pp.2537-2540 (1993)

[8] Tahir, N. A. and Long, K. A., *Laser and Particle Beams*, **2** part3, pp.371-381 (1984)

[9] Brio, M. and Wu, C. C., *J. Comput. Phys*, **75**, pp400-422 (1988)